PHYSICAL REVIEW E **76**, 060301(R) (2007)

Spreading of a granular droplet

Iván Sánchez,[1] Franck Raynaud,[2] José Lanuza,[3] Bruno Andreotti,[3] Eric Clément,[3] and Igor S. Aranson[4]
[1]*Centro de Física, IVIC, AP 21827, Caracas 1020-A, Venezuela*
and Departamento de Física, Universidad Simón Bolívar, AR 89000, Caracas 1080-A, Venezuela
[2]*MSC, UMR 7057 (CNRS), Université Paris 7, 75013 Paris, France*
[3]*PMMH, UMR7636 (CNRS), ESPCI Université P6-P7, 10 Rue Vauquelin, 75005 Paris, France*
[4]*Materials Science Division, Argonne National Laboratory, Argonne, Illinois 60439, USA*
(Received 24 May 2006; revised manuscript received 12 July 2007; published 7 December 2007)

The influence of controlled vibrations on the granular rheology is investigated in a specifically designed experiment in which a granular film spreads under the action of horizontal vibrations. A nonlinear diffusion equation is derived theoretically that describes the evolution of the deposit shape. A self-similar parabolic shape (the"granular droplet") and a spreading dynamics are predicted that both agree quantitatively with the experimental results. The theoretical analysis is used to extract effective friction coefficients between the base and the granular layer under sustained and controlled vibrations. A shear thickening regime characteristic of dense granular flows is evidenced at low vibration energy, both for glass beads and natural sand. Conversely, shear thinning is observed at high agitation.

DOI: 10.1103/PhysRevE.76.060301 PACS number(s): 45.70.−n, 47.10.−g, 68.08.Bc, 47.57.Gc

I. INTRODUCTION

Granular matter is a model material presenting the phenomenology of a wide class of complex fluids with a yield stress governing the transition between solidlike and liquidlike behaviors. In this respect, the most important challenge is to establish microscopically founded constitutive relations describing the different phases as well as the features of the phase transition itself. In the last decade, various important propositions were made to draw analogies with glassy states of matter or out of equilibrium thermodynamics [1,2] and phase transitions [3,4], but a full understanding still remains an open question. An important reason has been the failure of classical rheometers, which do not lead to homogeneous flows [5]. For dense granular flows, the situation has progressed by the introduction of new geometries (Ref. [6], and references therein) such as the inclined plane configuration, in which the stress tensor is controlled. Now, it is known that sufficiently far from the jamming transition, the dense granular flow rheology is *local* in first approximation: it is governed by an effective friction coefficient increasing with the shear rate properly rescaled by the local confining pressure. The kinetic theory, valid in the gaseous regime, fails to describe this situation characterized by the existence of long term contacts and force networks. In particular, binary collisions lead to a decrease of friction [7] with the shear rate instead of the observed increase. The most important open issue concerns the jamming or unjamming transition and the lack of identification of parameters controlling this hysteretic transition [4]. It has recently been suggested that the dynamics in the metastable region could be dominated by elementary rearrangements, interacting nonlocally [8] by fluctuations or by the coupling with the modes of vibration [9] (from internal or external origin).

Here we have designed a specific experiment to measure the influence of controlled vibrations on the granular rheology. We hereafter study the unjamming induced by horizontal shaking due to the transfer of energy by friction. Note that all previous experiments have been performed in confined geometries. The majority of them have used vertical vibration to agitate granular matter but relatively few have used horizontal shear [10–13]; see also Ref. [14] for review. We focus on two different questions. How does a granular film spread under the action of horizontal vibrations? How can the rheology be deduced from the spreading dynamics?

II. SETUP

The experimental apparatus is a horizontally shaken tray [Fig. 1(a)] whose motion is a sinusoid of amplitude a and angular frequency $\omega=2\pi f$. Driving frequencies f is between 15 and 30 Hz and the maximum amplitude is 1mm. The substrate is a sand-cast aluminum plate with roughness of about 10 μm. The tray is stabilized by four ball-bearing rings gliding on two rails. The tray is leveled horizontally within $1/100°$. A charge couple device (CCD) video camera moves along with the tray and images the surface of the deposit. From the deviation of a laser sheet shined at a small angle $\sim 6°$, we extract by correlation the droplet profile $h(x,t)$ with a subpixellar resolution ($\delta h \sim 50$ μm). Two granular materials are used: glass beads of diameter $d=300\pm 50$ μm, whose static and dynamical friction coefficients are, respectively, $\mu_s=0.47$ and $\mu_d=0.43$ and faceted Fontainebleau sand ($d=300\pm 60$ μm, $\mu_s=0.66$, and $\mu_d=0.60$). The following protocol is used to prepare a layer with reproducible initial conditions: an initial mass of sand is poured in a rectangular bottomless confining box fixed to the substrate. The box inner base defines the initial width $L_x=40$ mm in the vibration direction x and $L_y=150$ mm in the lateral dimension. To level off the deposit, the granular material is shaken vigorously for 1 min at 40 Hz. After removal of the confining box, an initial rooflike shape sand layer is obtained [Fig. 1(b), top]. To keep a lateral confinement of the deposit, two small guiding sidewalls are fixed on the tray.

III. AN INERTIAL TRIBOMETER

When the vibration is switched on, the granular layer loses its stability, gets a smooth shape, and spreads horizon-

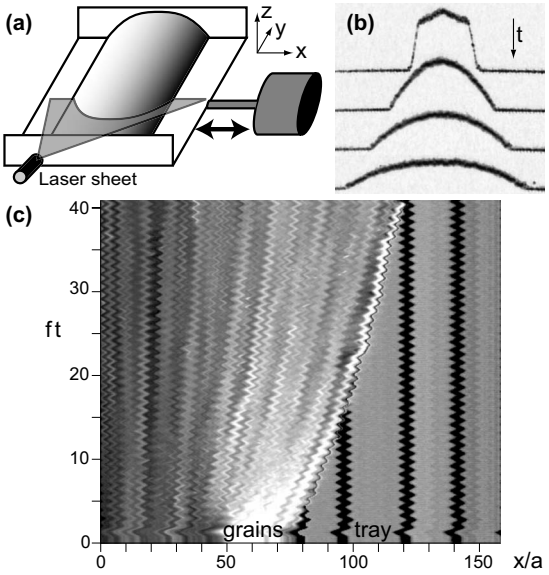

FIG. 1. (a) Sketch of the experimental setup. (b) Laser profile as a function of time: the top one corresponds to the granular film prior to shaking; the three below are subsequent deposit shapes after the vibration onset. Due to the laser inclination, the height is magnified by a factor $\simeq 10$. (c) Space-time diagram obtained with a fast video camera. The black sinusoids on the right show the tray motion. The trajectories on the left are directly that of surface grains. The white trace at the center shows the spreading granular front.

tally along the x direction [Fig. 1(b)]. From direct visualization of the layer motion [Fig. 1(c)], it can be observed that within an oscillation period, all the surface grains bear almost the same relative phase with respect to the plate. This suggests a close analogy with the motion of a solid slider. If a constant Coulomb static friction μ_s is assumed, the onset of relative motion between the substrate and the solid would correspond to a rescaled acceleration $\Gamma = a\omega^2/g$ equal to μ_s. Actually, the situation turns out to be more complex. We leave a systematic study of the motion onset to a future report and we focus here on the high Γ regime, starting from large deposit heights. Under these conditions, the film is set into motion and eventually leaves the limits of the tray before stoppage.

Let us consider the dynamics of a vertical slice of the granular droplet of width dx, of length L_y, and of height $h(x,t)$ [Fig. 1(c)]. Along the vertical direction, pressure P balances gravity g and reads: $P = \rho g(h-z)$, where ρ is the density of the material. Assuming normal stress isotropy, the pressure gradient induces a driving force $-L_y dx \rho g h \partial_x h$ on the slice. The tray exerts on it a resistive force $L_y dx \tau$ (τ is the shear component of stress) that opposes, on the average, the spreading motion. To assess the momentum transfer due to the complex sliding dynamics between the droplet and the base, we introduce a friction coefficient μ relating τ to P. It is worth noting that μ can depend on the basal pressure P, on h, a, and ω. The strong hypothesis is that it weakly depends on the relative velocity between the grains and the tray. We checked, for instance, that the introduction of a hysteresis between static and dynamic regimes does not affect significantly the results in the range of Γ investigated here.

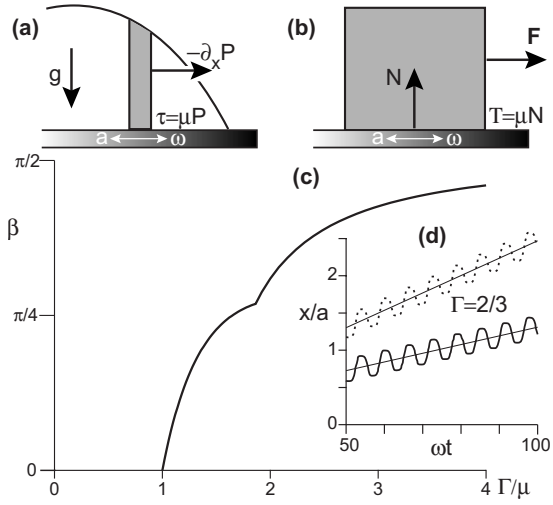

FIG. 2. (a) Forces acting on a vertical slice of the drop. (b) Analogy with a solid slider on a vibrating tray. (c) Function $\beta(\Gamma/\mu)$ relating the sliding velocity to friction [Eqs. (3) and (4)]. (d) Trajectories of a solid slider with respect to an oscillating tray for $\mu = 1/2$, $\Gamma = 2/3$, and for $F/N = 10^{-2}$ (solid line) and $F/N = 2 \times 10^{-2}$ (dotted line). The thin lines show the analytical prediction of the mean drift [Eq. (2)].

Then, the problem is completely similar to that of a solid block on an oscillating tray, submitted to a driving force F and a normal force $N = mg$ [Fig. 2(b)]. The analogy is established through the dimensionless parameter $F/N = -\partial_x h$. Our setup is in some sense the equivalent of the "inertial tribometer" [15] designed in the context of solid on solid friction studies. We make the equations of motion dimensionless using ω^{-1} as a characteristic time and a as a characteristic length. In the sliding regime, the equation governing the evolution of the dimensionless velocity difference v between the slider and the tray is

$$\Gamma \dot{v} = \Gamma \sin t - \mu \frac{v}{|v|} + \frac{F}{N}. \tag{1}$$

Blockage of motion occurs for $v = 0$. From rest (in the moving reference frame), motion starts when $|\sin t| = \mu/\Gamma$. We have obtained exact solutions of the problem at the linear order in F/N. For the purpose of the present paper, we only need the average sliding velocity $\bar{v}$, which is written under the form

$$\bar{v} = \frac{\beta[\Gamma/\mu]}{\mu} \frac{F}{N}. \tag{2}$$

Depending on the value of Γ/μ, the block motion may undergo two different dynamical regimes [Fig. 2(c)]: a continuously sliding at large acceleration, for which

$$\beta = \frac{\pi}{2} \sqrt{1 - \frac{\pi^2 \mu^2}{4\Gamma^2}}, \tag{3}$$

and stop or start motions at smaller acceleration, for which

$$\beta = \frac{\mu[\phi - \arcsin(\mu/\Gamma)]^2}{2\pi\Gamma}, \tag{4}$$

where ϕ is the root of the transcendental equation: $\cos(\phi)\Gamma/\mu + \phi = \sqrt{(\Gamma/\mu)^2 - 1} + \arcsin(\mu/\Gamma)$. β is an increasing function of Γ/μ that reflects the fraction of time during which the solid block slides [Fig. 2(d)]. To conclude this section, let us emphasize that the drag force varies linearly with the drift velocity although no viscosity is involved. This directly results from the interplay between inertia and solid friction.

IV. SPREADING DYNAMICS

A small aspect ratio H/W droplet allows for a depth integrated (Saint-Venant) description. Assuming no significant variation of density ρ, the flux of grains across a vertical section of the drop can be approximated by $a\omega\bar{v}h$. Using Eq. (2), the mass conservation law yields a nonlinear diffusion equation,

$$\partial_t h = \partial_x(U\partial_x h^2) \quad \text{with} \quad U = \frac{a\omega\beta(\Gamma/\mu)}{2\mu}. \tag{5}$$

Note that the diffusion coefficient U is velocity independent. Assuming that U does not depend on height h, Eq. (5) admits an exact parabolic self-similar solution as follows:

$$h(x,t) = \frac{3S}{2W(t)}\left[1 - \left(\frac{2x}{W(t)}\right)^2\right], \tag{6}$$

with a spreading dynamics that can be written as

$$W(t)^3 = W(0)^3 + 72SUt. \tag{7}$$

It can be shown that sufficiently localized initial conditions converge at long time toward the self-similar solution—just like the convergence toward Gaussians in linear diffusion. Experimentally, the profiles $h(x,t)$ were fitted by a parabola, allowing the determination of the width $W(t)$ and the maximal height $H(t)$ with a relative precision of 10^{-3}. Figure 3 shows the profiles measured at different times, rescaled by W and H. Remarkably, all experimental points collapse on the predicted parabolic shape [Eq. (6)]. Residuals of the difference between the fitted curve and the experimental data shows a deviation to a parabola of less than 4% in the central part and around 10% on the edges, for all data presented here. Compaction is small as the cross section area varies by less than 1% over time and is equal to $S = 2H(t)W(t)/3$.

Several curves $W(t)^3 - W(0)^3$ obtained for $f = 24$ Hz are displayed in Fig. 3(c). They present a quasilinear time dependence whose slope increases with the vibration amplitude a. We have chosen here initial width values $W(0)$ such as to avoid the nonuniversal initial transient. Note that in our experiment, because of the lateral boundaries, we have evidenced weak but systematic transverse curvatures—the central part spreads faster. Strictly speaking, the spreading dynamics is three-dimensional but may be approximated by a two-dimensional description since the curvature effect is weak. So, theoretical predictions of the shape [Eq. (6)] and the spreading law [Eq. (7)] are both in excellent agreement with experimental findings (Fig. 3).

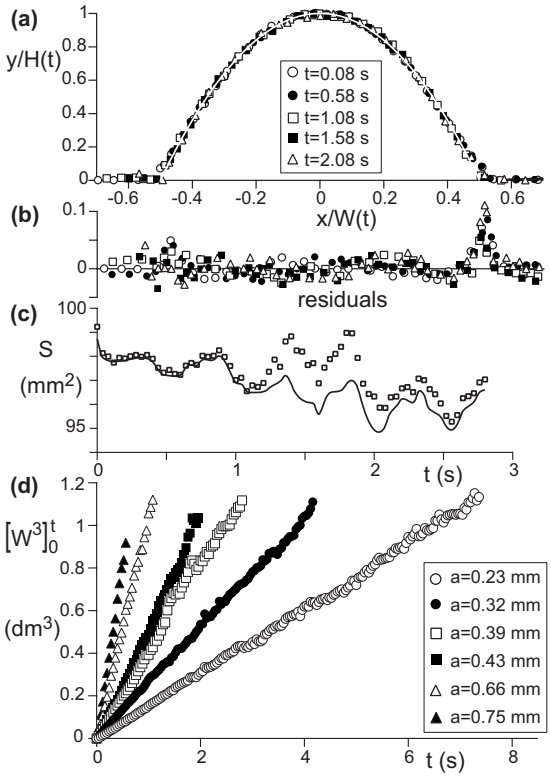

FIG. 3. Spreading dynamics for sand at $f = 24$ Hz. (a) Rescaled droplet shapes at different times t for $a = 0.39$ mm. (b) Fit residuals. (c) Droplet surface S as a function of time, computed by integration (solid line) or approximated by $2H(t)W(t)/3$ (□). (d) $W(t)^3 - W(0)^3$ for various a.

V. EFFECTIVE RHEOLOGY

Using Eqs. (5) and (7), the slope of the relation between W^3 and time t can be written as

$$\frac{dW^3}{dt} = \frac{18gS}{\pi f}\frac{\Gamma}{\mu}\beta(\Gamma/\mu). \tag{8}$$

From this relation, we have extracted an effective friction coefficient μ_{eff} from the local slope of $W(t)^3$ over a moving 1 s time window, with a systematic error smaller than 0.02. For large heights (say $H/d > 10$ for sand and $H/d > 5$ for glass beads), the variations over time of μ_{eff} are smaller than 0.05. Now, μ_{eff} varies from one experiment to the other by ~ 0.03 for glass beads and ~ 0.1 for sand. Therefore, as initially desired, this spreading experiment allows one to perform explicit measurements of a granular rheology under controlled vibration with 10% resolution.

Figure 4 shows the effective friction coefficient μ_{eff} as a function of the rescaled vibration velocity $I = \frac{a\omega}{\sqrt{gd}}$, which nicely collapses our data. This parameter is somehow similar to the inertial number I built in the context of sheared dense granular flows [4,6]: it compares the shear velocity at the scale of the grain (here $a\omega$) and the typical impact velocity.

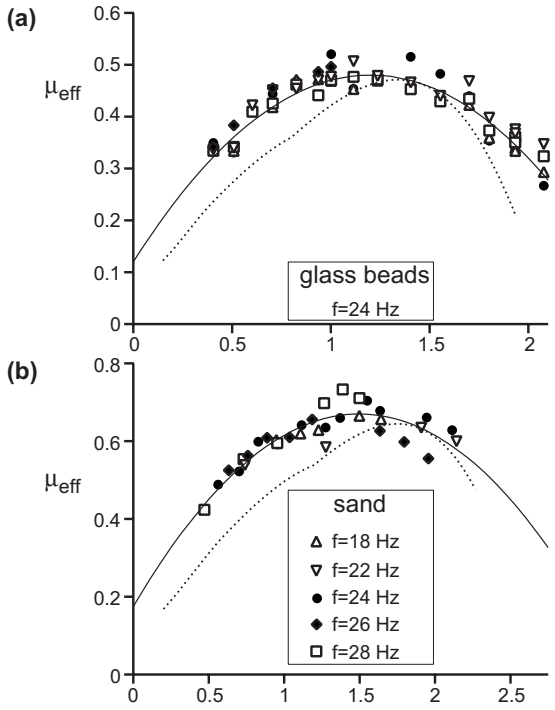

FIG. 4. Effective friction μ_{eff} as a function of the rescaled vibration velocity $I=a\omega/\sqrt{gd}$. The solid line is the best fit by a parabola. The dashed line is the test of consistency of the solid-block model with a velocity dependent friction (see the text). (a) Sand. Best fit: $\mu_{\text{eff}}(I)=0.67-0.22(I-1.5)^2$. (b) Glass beads ($f=24$ Hz). Best fit: $\mu_{\text{eff}}(I)=0.48-0.25(I-1.2)^2$.

However, it is important to note that, here, this characteristic velocity is $\sqrt{gd}$, which corresponds to a free fall from a grain size, and not to $\sqrt{P/\rho}\sim\sqrt{gh}$. Our experimental resolution—as well as the presence of a maximum in $\mu_{\text{eff}}(I)$—allows one to dismiss the later possibility.

Moreover, as a test of consistency, we checked in the block model that if we assume a friction coefficient μ depending on the instantaneous sliding velocity v as $\mu=\mu_{\text{eff}}[v/\sqrt{gd}]$, where μ_{eff} is the experimental law (Fig. 4, solid line), we recover a nonmonotonic curve for the effective friction coefficient determined from the drift velocity through the function β (Fig. 4, dashed line). Of course, both values do not need to correspond exactly since the passage from local to global friction is a nontrivial issue but this calculation shows that the existence of a maximum is indeed a robust feature of the model.

In the whole range of parameters, the coefficient μ_{eff} remains within 50% of the dynamical friction coefficient μ_d. Furthermore, its value for sand is higher than that for glass beads in the ratio of μ_d or μ_s. This makes us confident about the interpretation of μ_{eff} as a real friction coefficient. For both sand and glass beads, the resolution achieved with our apparatus is sufficient to evidence a nonmonotonous variation of friction with agitation. At large I, a weakening regime is evidenced that corresponds to a shear thinning behavior, characteristic of the predictions of kinetic theory [7]. Conversely, at low I, we evidence a robust shear thickening rheology, which is reminiscent from the behavior of dense granular flows [4,6]. In further studies, it will be crucial to investigate the jamming transition in this "inertial tribometer" in the regime of small Γ and/or small heights H/d.

ACKNOWLEDGMENTS

We thank A. Roussel and F. Naudin for introducing us to the industrial problem and the Tarkett-Sommer Company for financial help. A. Fornari has done some of the measurements presented here. I.S.A. was supported by US DOE, Office of Science, Contract No. DE-AC02-06CH11357. I.S. was supported by PCP Franco-Venezuelan Contract "Dynamics of granular materials."

[1] A. Liu and S. R. Nagel, Nature (London) **396**, 21 (1998).
[2] H. A. Makse and J. Kurchan, Nature (London) **415**, 614 (2002).
[3] I. S. Aranson and L. S. Tsimring, Phys. Rev. E **64**, 020301(R) (2001); D. Volfson, L. S. Tsimring, and I. S. Aranson, Phys. Rev. Lett. **90**, 254301 (2003).
[4] B. Andreotti, Europhys. Lett. **79**, 34001 (2007).
[5] N. Huang, G. Ovarlez, F. Bertrand, S. Rodts, P. Coussot, and D. Bonn, Phys. Rev. Lett. **94**, 028301 (2005).
[6] G. D. R. Midi, Eur. Phys. J. E **14**, 341 (2004).
[7] M. Y. Louge, Phys. Fluids **13**, 1213 (2001).
[8] A. Kabla and G. Debregeas, Phys. Rev. Lett. **90**, 258303 (2003).
[9] F. Dalton, F. Farrelly, A. Petri, L. Pietronero, L. Pitolli, and G. Pontuale, Phys. Rev. Lett. **95**, 138001 (2005).
[10] G. Metcalfe, S. G. K. Tennakoon, L. Kondic, D. G. Schaeffer, and R. P. Behringer, Phys. Rev. E **65**, 031302 (2002).
[11] C. Saluena and T. Poeschel, Eur. Phys. J. E **1**, 55 (2001).
[12] M. Medved, H. M. Jaeger, and S. R. Nagel, Europhys. Lett. **52**, 66 (2000).
[13] P. M. Reis and T. Mullin, Phys. Rev. Lett. **89**, 244301 (2002).
[14] I. S. Aranson and L. S. Tsimring, Rev. Mod. Phys. **78**, 641 (2006).
[15] T. Baumberger, L. Bureau, M. Busson, E. Falcon, and B. Perrin, Rev. Sci. Instrum. **69**, 2416 (1998).